Strength of Partially Frozen Sand Under Triaxial Compression

Yawu Liang, Nicholas Beier & D.C. Sego
Geotechnical Center, Department of Civil & Environmental Engineering, University of Alberta, Edmonton, AB T6G 2G7, Canada

GeoCalgary 2022 October 2-5 Reflection on Resources

ABSTRACT
To investigate the effect of pore matrix (ice and water) on the strength of partially frozen sand, a series of triaxial compression tests with internal pore water pressure measurements were performed. Both dense and loose saline sand samples were prepared by rapidly freezing the samples and then slowly warming to and subsequently shearing at -3 ºC. Compared with unfrozen sand, the temperature only affects the effective cohesion not the effective friction angle in dense sand. Based on Ladanyi and Morel's (1990) concept of internal confinement on the frozen sand, a Mohr–Coulomb model that uses effective failure and residual angles from unfrozen sand to estimate the strength of partially frozen sand is presented. The proposed model reflects how the pore matrix contributes to the strength of partially frozen sand. For loose sand, the peak strength is enhanced by the internal confinement and cohesion resulting from the pore water (suction) and pore ice respectively. For dense sand, only pore ice affects the peak strength by adding the internal confinement and cohesion.

RÉSUMÉ
Pour étudier l'effet de la matrice des pores (glace et eau) sur la résistance du sable partiellement gelé, une série d'essais de compression triaxiale avec des mesures de la pression interstitielle interne a été effectuée. Des échantillons de sable salin dense et meuble ont été préparés en congelant rapidement les échantillons, puis en les réchauffant lentement jusqu'à -3 ºC et puis en les cisaillant à cette température. Par rapport au sable non gelé, la température n'affecte que la cohésion effective et non l'angle de frottement effectif dans le sable dense. Basé sur le concept de confinement interne de Ladanyi et Morel (1990) sur le sable gelé, un modèle Mohr-Coulomb qui utilise la rupture effective et les angles résiduels du sable non gelé pour estimer la résistance du sable partiellement gelé est présenté. Le modèle proposé reflète la façon dont la matrice des pores contribue à la résistance du sable partiellement gelé. Pour le sable meuble, la résistance maximale est renforcée par le confinement interne et la cohésion résultant respectivement de l'eau interstitielle (succion) et de la glace interstitielle. Pour le sable dense, seule la glace interstitielle affecte la résistance maximale en ajoutant le confinement interne et la cohésion.

1 INTRODUCTION

Projected climatic change will gradually warm "near surface" permafrost so the soil is in a partially frozen state due to the coexistence of unfrozen water and ice phases in the pores. Consequently, infrastructure built on these areas will become more vulnerable, which has a significant impact on coastal and northern communities. Compressive strength of frozen soil is an important mechanical property in design and evaluation of structures in cold regions. Therefore investigating the effect of internal stresses from unfrozen water and pore ice on the strength of partially frozen soil is important.

Since ice can sustain both hydrostatic and deviator stresses, the mechanical behavior of frozen soil is strongly affected by the pore ice. The behavior of polycrystalline ice is greatly dependent on the strain rate: it shows a ductile response at lower strain rates but turns into a brittle manner as strain rate increases (Mellor 1979). This transition marked by strain rate is governed by stress state, temperature and grain-size (Kalifa et al. 1992). For loose or ice-rich sand, the behavior and measured strength were similar to that of polycrystalline ice (Goughnour and Andersiand 1968). However, when the sand becomes denser, both ice strength and internal confinement due to the dilatancy hardening contribute to the overall strength (Ladanyi and Morel 1990). To evaluate the effect of internal confinement on strength of frozen dense sand, Ladanyi and Morel (1990) proposed following equation:

$$q_{FS} = (\sigma_{3cell} + T_i)(K'_p - 1) + q_i \quad [1]$$

Where

q_{FS} is the peak strength of frozen sand;

σ_{3cell} is the cell pressure;

T_i is the tensile stress provided by pore ice due to the dilatancy hardening;

$$K'_p = \tan^2(45 + \emptyset'/2) \quad [2]$$

is the passive earth pressure coefficient and $\emptyset'$ is the effective friction angle; and

q_i is the shear strength of polycrystalline ice.

The effective friction angle can be determined from unfrozen dense samples under drained or undrained condition as the solid contact is still predominated by grain particles in the frozen state and hence the pore ice does not affect the friction angle of sand (Alkire and Andersland 1973; Sayles 1974). This theoretical model is limited to the frozen dense sand where the unfrozen water is negligible,

therefore its application to the partially frozen sand needs further investigation.

Unfrozen water would be another major factor influencing the behavior of frozen soil if the temperature is not cold enough for ice to fill the majority of pore space. The strength of frozen soil will decrease as the unfrozen water content increases with warming temperatures and salinity (Ogata et al. 1983; Stuckert and Mahar 1984; Pharr and Merwin 1985; Hivon and Sego 1995; Xu et al. 2017). On the other hand, when there is sufficient unfrozen water to form a continuous water phase within partially frozen soil, measuring pore-water pressure (PWP) and establishing the internal effective stress and its impact on the mechanical behavior are necessary. However, limited research has been reported. Recently, Arenson and Springman (2005) measured PWP in ice-rich samples under triaxial conditions, Lyu et al. (2021) investigated the PWP response in the frozen saline clay under different temperatures and strain rates. But continuity of the internal water phase was not established by Arenson and Springman (2005) and Lyu et al. (2021), which is a prerequisite to obtain true PWP throughout the entire sample. Kia (2012) confirmed continuity of the internal water phase and then measured PWP using 5 Filter-less Rigid Piezometers (FRPs) within the partially frozen sand, but these tests were restricted to one-dimension no lateral yield conditions.

Although there is a challenge in measuring internal stresses within the pore matrix (ice and water) directly, this study attempted to investigate the individual effect of each component of the pore matrix on the strength of partially frozen sand. A series of triaxial compression tests were performed using dense and loose sand with 30 ppt pore fluid salinity. The specimens were prepared by rapidly freezing and then slowly warming the specimens to and subsequently shearing them at -3 ^{o}C. Based on Ladanyi and Morel's (1990) concept of internal confinement within frozen sand, a simple model for estimating the strength of partially frozen sand is presented.

2 MATERIAL AND METHODS

2.1 Material

The tests were carried on 100 mm diameter and 196 mm high specimens of a uniformly graded fine sand with a salinity of 30 ppt (30 g/L) that represents high-salinity pore fluid found beneath arctic coastal communities (Hivon and Sego 1993). The specific gravity is 2.64 and the grain sizes vary from 0.15 mm and 0.85 mm (D_{50} = 0.28 mm).

2.2 Test Apparatus

As shown in Figure 1, a new triaxial apparatus was developed from a modified test cell to measure internal PWP within the soil while maintaining the thermal boundary conditions involved in a partially frozen test (Liang et al. 2022). Two cold baths were used to control the cell temperature by circulating water-glycol mixture (1:1) through a spiral copper coil inside the cell and the base cooling plate, respectively. Three thermistors attached on top, middle and bottom surface (membrane) of the specimen were utilized to monitor the temperature throughout the specimen. The base pressure transducer and three filter-less rigid piezometers (FRPs) embedded within the specimen were used to measure the internal PWP and confirm continuity of the water phase within the specimen.

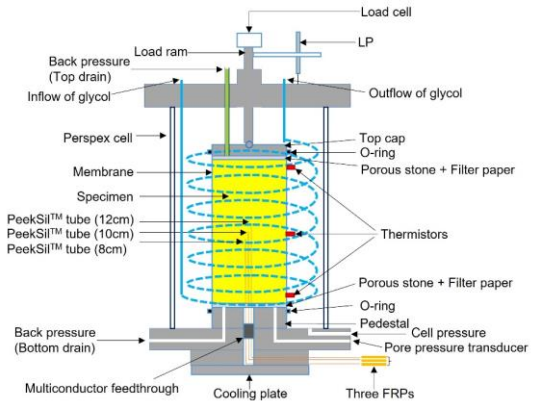

Figure 1. Schematic of apparatus (modified from Liang et al. 2022)

2.3 Test Procedures

The whole testing program included three unfrozen dense specimens, five partially frozen loose specimens and three partially frozen dense specimens (Table 1). Loose and dense specimens were reconstituted by moist tamping and slurry deposition methods, respectively. Then the specimens were saturated and consolidated to the targeted effective stress using the procedures described by Liang et al. (2022). Unfrozen tests were performed at a room temperature of 23 ^{o}C. After consolidation, specimens were sheared under undrained condition at the strain rate of 1 % per minute to determine effective friction angle at failure.

The triaxial apparatus was placed in a cold room with temperature to approximately 2 ^{o}C to carry out partially frozen tests. To provide enhanced temperature control, fiberglass insulation covered the cell surface and a foam board insulation box was placed around the cell. Partially frozen samples were prepared using five stages followed with consolidation: (1) First the specimen was frozen unidirectionally by circulating liquid nitrogen through the base cooling plate for about 7 h followed by a circulation of water-glycol mixture (-25 ^{o}C) from cold bath for a 12 h, with free drainage at the top (back pressure line). (2) Then the specimen was maintained around -11 ^{o}C using a cold bath (A) set at -11 ^{o}C connected to the spiral copper coil and another cold bath (B) attached to base cooling plate at -15 ^{o}C. (3) The temperature of cold bath (A) was set to -3 ^{o}C and maintained for approximately 36 to 42 h to warm the specimen uniformly to -3 ^{o}C and to stabilize the internal temperature. Top drainage line was frozen in the last stage, so it was switched to the bottom drainage line. The cold bath (B) was first raised to 1 ^{o}C for several hours until the drainage line thawed and then lowered to -2.5 ^{o}C to

minimize temperature gradient within the specimen. For these stages, the back pressure (400 kPa) and cell pressure remained the same following consolidation. (4) Confirm continuity of the water phase by increasing the back pressure independent of the applied cell pressure and measuring the corresponding increase in pore pressure measured by the base transducer and the internal FRPs (Kia 2012). If all measured PWP reflect the back pressure and show the same response, the internal waste phase is continuous. (5) Finally, the specimen was sheared at a constant strain rate (1%/min or 0.1%/min) while maintained at the test temperature.

Table 1. Summary of the testing program

Test ID	Initial Void Ratio	Stain rate (%/min)	Confining Pressure (kPa)	T (°C)
D-1	0.599	1	100	23
D-2	0.599	1	200	23
D-3	0.597	1	400	23
PL-1	0.835	1	100	-3
PL-2	0.834	1	200	-3
PL-3	0.835	1	400	-3
PL-4	0.834	0.1	100	-3
PL-5	0.835	0.1	400	-3
PD-1	0.596	1	100	-3
PD-2	0.599	1	200	-3
PD-3	0.594	1	400	-3

Note: D, unfrozen dense; PL, partially frozen loose; PD, partially frozen dense.

3 RESULTS AND DISCUSSION

3.1 Stress and PWP Response of Partially Frozen Samples

The stress and PWP response of partially frozen loose and dense sand are shown in Figure 2. There were some erratic measurements in PWP associated with blockage of the tube during the tests, so only validated continuity of PWP measurements were plotted for analysis. The behavior of partially frozen loose sand was ductile and peak strengths were similar to that of saline ice reported by (Melton and Schulson 1997). A continuous decrease of PWP displayed in partially frozen loose sand indicated that dilatancy occurred in pore space. Since no shear plane formed after failure, this shear-induced dilation was more likely caused by pore ice. Compared to samples tested at higher strain rate (1 % /min), both stress and PWP curves of samples at lower strain rate exhibited an apparent hysteresis and ended at a lower stress and suction. In contrast, partially frozen dense samples showed the same dilative response as unfrozen dense samples and an apparent shear plane presented during the tests, suggesting that its behavior was still mainly controlled by the particles making up the soil skeleton.

According to the definition, the effective stress is the difference between total stress and PWP, which controls the deformation and strength of soil, so the ice-soil system is treated as a solid phase in partially frozen soil (Blanchard and Fremond 1985; Ghoreishian et al. 2016). With continuity of PWP measurements, the effective stress paths of partially frozen samples are plotted in Figure 3. The effective stress paths of partially frozen loose samples converged independent of confining pressures but showed different slopes at different strain rates (Figure 3a), which reflected the strain rate-dependency of pore ice. Despite a clear distinction in the range of close to and after peak stress, the effective stress paths of partially frozen loose and dense samples were very close at initial stage (Figure 3b), possibly because the initial behavior of partially frozen dense samples were also primarily dependent on the pore ice. It is worth noting that both sets of effective stress paths ended up with the same ultimate line, indicating they had the same flow structure after failure. A comparison of effective stress paths between partially frozen loose samples and unfrozen dense samples are also presented (Figure 4). Two sets of effective stress paths were nearly identical before the peak stress at the same confining pressure. This means the pore ice that surrounds the soil grain brings the sand into a denser state, thus acquiring the similar macroscopic behavior like unfrozen dense sand.

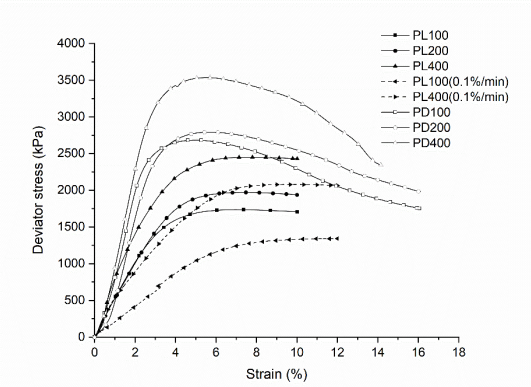

(a) Stress

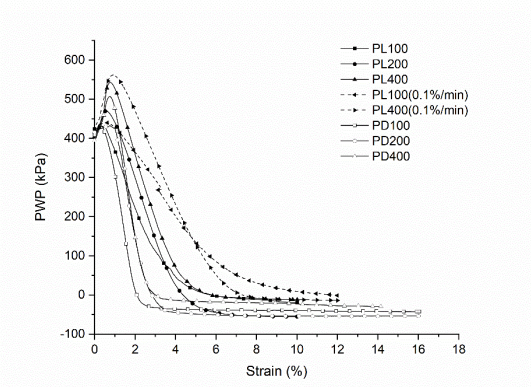

(b) PWP

Figure 2. Stress and PWP response of partially frozen sand

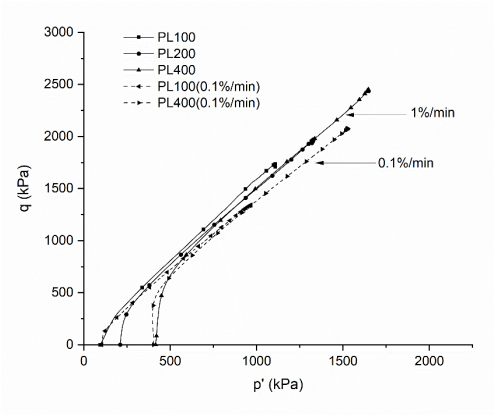

(a) Partially frozen loose sand (1% & 0.1%/min)

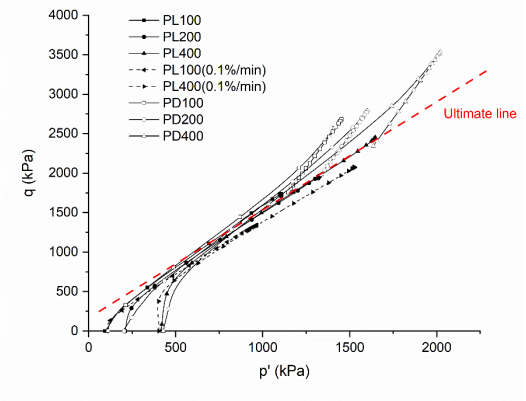

(b) Comparison of partially frozen loose and dense sand

Figure 3. Stress path of partially frozen sand

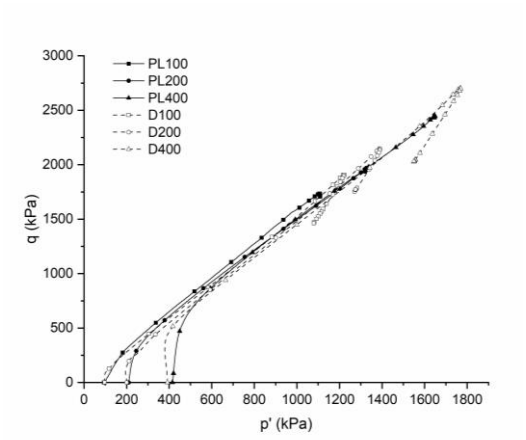

Figure 4. Comparison of stress path between partially frozen loose sand and unfrozen dense sand (1%/min)

3.2 Strength of Partially Frozen Samples

The strengths of unfrozen dense sand and partially frozen sand are summarized in Figure 5. The peak strength was defined at the maximum deviator stress sustained by the sample while the residual strength was determined at the end of the test. The peak and residual strength of partially frozen loose sand were very close, so only the peak strength was used for comparison. It can be seen that unfrozen and partially frozen dense samples have similar slopes but different interceptions of failure lines (peak strength), which means the temperature or pore ice only affects the effective cohesion instead of the effective friction angle in dense sand similar to what is found in frozen dense sand (Alkire and Andersland 1973; Xu et al. 2016; Xu et al. 2017). Similarly, the failure line of partially frozen loose sand had a similar slope to the ultimate line (residual strength) of unfrozen dense sand, giving alternative evidence that partially frozen loose sand had analogous mechanical property to that of unfrozen dense sand. Additionally, the residual strength of partially frozen dense sand was approximately equal to the peak strength of partially frozen loose sand under the same confining pressure. Peak strengths of partially frozen loose samples at lower strain rate lied on the ultimate line of unfrozen dense samples, suggesting that the effect of the ice matrix decayed away and created additional contacts between soil grains (Sayles 1974). It should be mentioned that the ultimate line of unfrozen dense samples should be the same as that of unfrozen loose samples. Further, this provides an insight to estimate the strength of partially frozen soil based on the unfrozen soil.

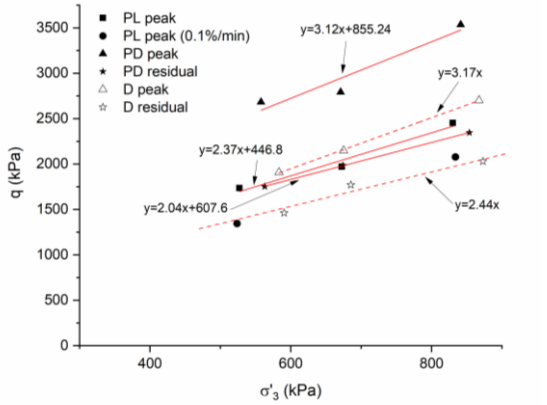

Figure 5. Strength of partially frozen sand and unfrozen dense sand

3.3 Proposed Model and Verification

According to the model established by Ladanyi and Morel (1990) and these experimental results, the proposed model is based on the following assumptions.

(1) In a partially frozen loose sand, the internal confinement resulting from tension or suction is solely generated via the pore water due to dilation of pore ice as it is sheared.

(2) In a partially frozen dense sand, the tension or suction caused by the dilation of soil skeleton is generated and shared by the pore water and pore ice, but only the

tensile stress sustained by pore ice is considered as internal confinement adding to the sand skeleton and it equals to the measured suction in the pore water.

As mentioned in the foregoing, the effective failure angle of partially frozen loose sand is close to the effective residual angle of unfrozen dense samples, thus the peak strength of partially frozen loose sand at strain rate of 1%/min will be

$$q_{PLS} = (\sigma_{3cell} + T_w)\tan\beta' + c_L \quad [3]$$

Where

q_{PLS} is the peak strength of partially frozen loose sand;

σ_{3cell} is the cell pressure;

T_w is the measured suction of pore water;

β' is the angle of ultimate line or effective residual angle of unfrozen dense sand; and

c_L is the cohesion caused by pore ice, which is the function of temperature and strain rate and determined from partially frozen loose sand.

The residual strength of partially frozen dense sand can also be predicted using Eq. 3, because it has almost the same value as the peak strength of partially frozen loose sand.

When the strain rate is less than 0.1%/min, the ice cohesion decreases due to creep and c_{iL} would be zero, therefore the peak strength of partially frozen loose sand at lower strain rate becomes

$$q_{PLS(low)} = (\sigma_{3cell} + T_w)\tan\beta' \quad [4]$$

Where

$q_{PLS(low)}$ is the peak strength of partially frozen loose sand at lower strain rate;

In the same way, the peak strength of partially frozen dense sand is given by

$$q_{PDS} = (\sigma_{3cell} + T_i)\tan\alpha' + c_D \quad [5]$$

Where

q_{PDS} is the peak strength of partially frozen dense sand;

T_i is the tensile stress of pore ice, which is equal to the measured suction of pore water;

α' is the angle of failure line or effective failure angle of unfrozen dense sand; and

c_D is also the cohesion caused by pore ice but determined from partially frozen dense sand.

Table 2. Summary of measured and predicted strengths

Test ID	PWP at Peak Strength (kPa)	Measured Peak Strength (kPa)	Predicted Peak Strength (kPa)
PL-1	-8	1735	1734
PL-2	-53	1970	2088
PL-3	-8	2451	2473
PL-4	-5	1345	1278
PL-5	-12	2079	2035
PD-1	-37	2684	2623
PD-2	-51	2793	2982
PD-3	-17	3536	3522

Note: Negative PWP refers suction.

Table 2. Continued

Test ID	PWP at Residual Strength (kPa)	Measured Residual Strength (kPa)	Predicted Residual Strength (kPa)
PL-1	-	-	-
PL-2	-	-	-
PL-3	-	-	-
PL-4	-	-	-
PL-5	-	-	-
PD-1	-42.7	1753.3	1821
PD-2	-53.8	1983.9	2092
PD-3	-29.5	2346.2	2530

In this case, the effective angle α', β' and cohesion c_L, c_D are 72.49°, 67.68°, 447 kPa and 855 kPa at the temperature of -3 °C (Figure 5), respectively. The PWP at peak and residual strength is presented in Table 2. According to Figure 6, the proposed model reflects the measured strength of partially frozen sand. Therefore, the strength of partially frozen sand can be expressed in a form of Mohr–Coulomb criterion, provided effective failure and residual angles are determined from unfrozen sand. Irrespective of the difference in PWP at peak or residual strength, conducting a partially frozen loose or dense sample along with PWP measurement is able to estimate the cohesion associated with pore ice and then predict strengths of other samples at different confining pressures. The model could explain that the suction measured in pore water affects strength of partially frozen loose sand by increasing the confining pressure, while pore ice influences the effective cohesion at higher strain rate. It also shows how the pore ice affects the peak strength of partially frozen dense sand by adding an internal confining pressure and the cohesion. Although the model is validated, it is limited to the current testing conditions, such as the temperature, stress level and salinity. Further investigation is required to examine the model under other situations.

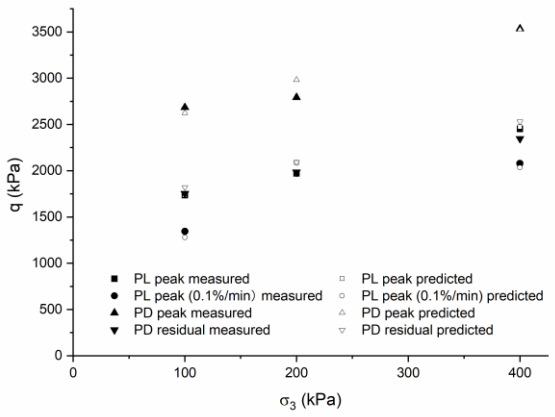

Figure 6. Verification of model

4 CONCLUSION

This paper presents the results of a series of triaxial compression tests on loose and dense sand at -3 °C to investigate the effect of pore matrix (unfrozen water and ice) on the strength of partially frozen sand. Followed by Ladanyi and Morel's (1990) concept of internal confinement on frozen sand, a modified model for estimating the strength of partially frozen sand is proposed and validated. The following main conclusions can be drawn from this study:

(1) The behavior of partially frozen loose and dense sand is mainly controlled by pore ice and soil skeleton respectively.

(2) The temperature or pore ice only affects effective cohesion not the effective friction angle in dense sand.

(3) At lower strain rate, the effect of ice matrix decreases via creep and the partially frozen loose sand has a similar effective residual angle as the unfrozen sand.

(4) The proposed model provides a bridge between the unfrozen and partially frozen sand in a form of Mohr–Coulomb criterion.

(5) For partially frozen dense sand, the peak stress is strengthened by the internal confinement and cohesion resulting from pore ice. However, the internal confinement that enhances the strength of partially frozen loose sand is generated from pore water via suction.

5. ACKNOWLEDGEMENT

The authors would like to acknowledge technological staff Lucas Duerksen and Christine Hereygers, from UofA Geotechnical Center, Department of Civil and Environmental Engineering, University of Alberta, for assistance in design and construction of the apparatus. We also thank Dr. Louis Kabwe from UofA Geotechnical Center for the help with French version of the abstract. The financial support of China Scholarship Council (CSC) and provided by the Natural Sciences and Engineering Research Council of Canada (NSERC) Discovery Grant Program (RGPIN-2019-04573) are gratefully acknowledged.

6 REFERENCES

Alkire, B.D., and Andersland, O.B. 1973. The effect of confining pressure on the mechanical properties of sand–ice materials. Journal of Glaciology, 12(66): 469-481.

Arenson, L.U., and Springman, S.M. 2005. Triaxial constant stress and constant strain rate tests on ice-rich permafrost samples. Canadian Geotechnical Journal, 42(2): 412-430.

Blanchard, D. and Fremond, M. 1985. Soil frost heaving and thaw settlement. In Proceedings of the 4th international symposium on ground freezing, Boca Raton, FL, pp. 209–216.

Ghoreishian Amiri, S. A., Grimstad, G., Kadivar, M. and Nordal, S. 2016. Constitutive model for rate-independent behavior of saturated frozen soils. Canadian Geotechnical Journal, 53(10): 1646–1657.

Goughnour, R.R., and Andersland, O. 1968. Mechanical properties of a sand-ice system. Journal of the Soil Mechanics and Foundations Division, 94(4): 923-950.

Hivon, E., and Sego, D. 1993. Distribution of saline permafrost in the Northwest Territories, Canada. Canadian Geotechnical Journal, 30(3): 506-514.

Hivon, E., and Sego, D. 1995. Strength of frozen saline soils. Canadian Geotechnical Journal, 32(2): 336-354.

Kalifa, P., Ouillon, G., and Duval, P. 1992. Microcracking and the failure of polycrystalline ice under triaxial compression. Journal of Glaciology, 38(128): 65-76.

Kia, M. 2012. Measuring Pore-water Pressure in Partially Frozen Soils. Ph.D. thesis, Faculty of Graduate Studies and Research, University of Alberta, Edmonton, AB.

Ladanyi, B., and Morel, J.-F. 1990. Effect of internal confinement on compression strength of frozen sand. Canadian Geotechnical Journal, 27(1): 8-18.

Liang Y, Beier N, and Sego DC. 2022. New Method for Internal Pore-Water Pressure Measurements. Geotechnical Testing Journal, 45(2): 490-502.

Lyu, C., Nishimura, S., Amiri, S.A.G., Zhu, F., Eiksund, G.R., and Grimstad, G. 2021. Pore-water pressure development in a frozen saline clay under isotropic loading and undrained shearing. Acta Geotechnica, 16(12): 3831-3847.

Mellor, M. 1980. Mechanical properties of polycrystalline ice. In Physics and Mechanics of Ice, International Union of Theoretical and Applied Mechanics, Copenhagen, Springer Verlag, Berlin, pp. 217-245.

Melton, J.S., and Schulson, E.M. The ductile deformation of columnar (S2) saline ice under triaxial compression. In The Seventh International Offshore and Polar Engineering Conference. 1997. OnePetro.

Ogata, N., Yasuda, M., and Kataoka, T. 1983. Effects of salt concentration on strength and creep behavior of artificially frozen soils. Cold Regions Science and Technology, 8(2): 139-153.

Pharr, G., and Merwin, J. 1985. Effects of brine content on the strength of frozen Ottawa sand. Cold regions science and technology, 11(3): 205-212.

Sayles, F.H. 1974. Triaxial constant strain rate tests and triaxial creep tests on frozen Ottawa sand. Corps of Engineers, US Army Cold Regions Research and Engineering Laboratory. Technical Report 253.

Stuckert, B., and Mahar, L. Role of ice content in the strength of frozen saline coarse grained soils. In Proceedings, Cold Regions Engineering Specialty Conference, Edmonton, AB. Montreal: Canadian Society for Civil Engineering. 1984. pp. 579-587.

Xu, J., Liu, H., and Zhao, X. 2017. Study on the strength and deformation property of frozen silty sand with NaCl under tri-axial compression condition. Cold Regions Science and Technology, 137: 7-16.

Xu, X., Wang, Y., Bai, R., Fan, C., and Hua, S. 2016. Comparative studies on mechanical behavior of frozen natural saline silty sand and frozen desalted silty sand. Cold Regions Science and Technology, 132: 81-88